Motor and non-motor symptoms in cervical dystonia

Smit, Marenka

CHAPTER 6

Indications of an altered serotonergic state in cervical dystonia: a [^{11}C]DASB PET study

M Smit
D Vállez García
BM de Jong
RA Dierckx
AT Willemsen
EF de Vries
AL Bartels
MA Tijssen

Submitted.

ABSTRACT

Background: The pathophysiology of cervical dystonia (CD) is largely unknown. Regarding the involvement of neurotransmitter changes, the serotonergic system has been implicated in dystonia. In this imaging study we aimed to assess whether altered presynaptic serotonin transporter (SERT) binding contributes to the CD pathophysiology, concerning both motor and non-motor symptoms (NMS).

Methods: We studied the non-displaceable binding potential (BP_{ND}) of SERT using [^{11}C] DASB PET imaging in 14 CD patients and 12 age- and gender-matched controls. Severity of motor symptoms was scored using the TWSTRS and CGI-S jerks/tremor scale. NMS depression, anxiety, fatigue and sleep disturbances were assessed with quantitative rating scales. The correlation between SERT binding and clinical patient characteristics was analyzed with the Spearman's rho test and multiple regression.

Results: Increased BP_{ND} in the dorsal raphe nucleus significantly correlated ($p<0.001$) with motor symptom severity (r_s=0.65), pain (r_s=0.73) and sleep disturbances (r_s=0.73), with motor symptom severity being the most important predictor. Compared to controls, the increased dRN binding in patients was not significant (18.3%, d=0.46, p=0.21).

An opposite trend of BP_{ND} binding was particularly found in the putamen of CD patients (right 10.7%, d=0.64, p=0.06; left 8.8%, d=0.57, p=0.11) which, however, did not correlate with clinical parameters.

Conclusion: Emphasizing the clinical correlation with enhanced [^{11}C]DASB binding in the dRN, we propose that CD is associated with an enhanced state of serotonergic activity. The consequent increase of distant endogenous serotonin release inflicts a reduction of striatum [^{11}C]DASB binding due to competition between serotonin and [^{11}C]DASB.

INTRODUCTION

Cervical dystonia (CD) is a movement disorder characterized by involuntary abnormal muscle contractions of the neck. Non-motor symptoms (NMS) like psychiatric features, pain and fatigue are prevalent in up to 95% of CD patients [1].

The pathophysiology of CD is largely unknown. Neurotransmitter changes have been suggested and the serotonergic system has been implicated in both motor and NMS in dystonia [2]. A dense projection of fibers from serotonergic neurons, located within the raphe nuclei in the brainstem, arise to important structures of the basal ganglia motor control system, such as the striatum and internal globus pallidus (GPi). The GPi plays a key role in the network underlying the dystonia pathophysiology [3,4], supported by the therapeutic effect of GPi deep brain stimulation for dystonia [3].

Positron emission tomography (PET) provides an unique opportunity to study the serotonin transporter (SERT), an important presynaptic marker of serotonergic functioning, *in vivo*. The PET radioligand [11C]DASB is a tracer to measure SERT binding in the human brain. In Parkinson's disease, [11C]DASB PET studies have shown that aberrations of SERT are related to both motor and NMS, including tremor severity [5], dyskinesia [6], fatigue [7] and depressive symptoms [8]. To the best of our knowledge, SERT binding has never been studied in dystonia patients.

In this study, we examined SERT binding in CD patients and matched controls using [11C]DASB PET imaging and corrected for the serotonin transporter gene-linked polymorphism. We hypothesized that dysfunction of the serotonergic system is a shared pathophysiological pathway for motor- and NMS in CD patients.

METHODS

Subjects

This case-control study included 14 patients with a clinically diagnosed idiopathic CD and 14 age- and sex-matched controls.

The number of subjects was based on numbers (between 10 and 15 subjects) described in [11C]DASB PET studies in the literature [5,7].

Exclusion criteria included onset of CD before the age 18 and severe tremor and/or jerks obstructing accurate brain imaging. Exclusion criteria for all subjects were other relevant neurological co-morbidity and the use of serotonergic medication or antidepressants. Informed consent was obtained from all participants and the study was approved by the local ethics committee.

Clinical measures

Motor assessment was performed using a systematic video protocol, within two weeks prior to or one week after botulinum toxin treatment in order to obtain the least influenced motor score. CD motor symptom severity and related pain were scored with the Toronto Western Spasmodic Torticollis Rating Scale (TWSTRS) [9]; severity of jerks and tremor were scored using the Clinical Global Impression Scale: CGI-S jerks-tremor [10]. Motor function was independently scored by two experts (MS, VH) and the average score was used in the statistical analysis as there was good inter-observer agreement (Intraclass Correlation Coefficients >0.70, two-way mixed, absolute agreement).

NMS, including depression, anxiety, fatigue and sleep disturbances, were assessed using the Beck Depression Inventory (BDI), the Beck Anxiety Inventory (BAI), the Fatigue Severity Scale (FSS) and the Pittsburgh Sleep Quality Index (PSQI) (see also Smit et al., [11]).

Genetics

The serotonin transporter gene-linked polymorphic region (5-HTTLPR), encoded by the *SLC6A4* gene, is an important regulator of the number of expressed serotonin transporters. Three different alleles in this polymorphic region have been associated with changes in transcriptional activity. Functionally, the S and L_G allele induce low transcriptional activity, while the L_A allele induce high transcriptional activity [12]. We classified 5-HTTLPR status as L_A/L_A genotype or L_G/S-allele carrier; details of the methodology are explained in the supplementary material.

PET and MRI data acquisition

Positron emission tomography imaging was performed either with a Biograph 40-mCT or 64-mCT (Siemens Healthcare, USA). Head movement was minimized with a head-restraining band. After a low-dose CT for attenuation and scatter correction, a dynamic 60-min data acquisition scan was started simultaneously to an intravenous bolus injection of [11C]-3-amino-4-(2-dimethylaminomethyl-phenylsulfanyl)benzonitrile ([^{11}C]DASB) (379±44 MBq). Synthesis of [^{11}C]DASB was performed by methylation of N-Methyl-2-(2-amino-4-cyanophenylthio)-benzylamine, details have been reported elsewhere [13].

Axial 3D T1-weighted gradient-echo images (3T Intera, Philips, The Netherlands) of the brain were acquired from all participants. MR images were visually examined and no structural lesions were detected.

Image reconstruction and preprocessing

The list-mode data from the PET scans was reconstructed using the 3D OSEM algorithm, (3 iterations and 24 subsets), point spread function correction and time-of-flight, resulting in a matrix of 400 × 400 × 111 of isotropic 2 mm voxels, smoothed with 2 mm filter at full width at half maximum, and 23 frames (7×10 sec, 2×30 sec, 3×1 min, 2×2 min, 2×3 min, 5×5 min, 2×10 min).

Image processing and pharmacokinetic analysis was performed with PMOD v3.7 software (PMOD Technologies Ltd, Switzerland). Motion correction was applied to the PET images (frame 9 to 23, using frame 15 as reference) to account for the movement of the subject during the scan. Then, the summed image (frames 13 to 23) was used for rigid matching registration of the individual PET to the individual MRI. A 3 tissue probability map normalization of the individual MRI into the Montreal Neurological Institute (MNI) standard space was calculated, and subsequently applied to the corresponding PET image [14].

Predefined volumes of interest (VOIs) (Supplementary table 1) were transformed back into individual space, based on the Hammers atlas [15] and limited to the grey matter tissue of cortical regions (>30% grey matter probability based on individual segmentations). In addition, VOIs for the dorsal raphe nucleus (dRN) and the median raphe nucleus (mRN) were manually defined based on their MNI coordinates (atlas based, i.e. dRNa and mRNa) [16]. Moreover, driven by local signal intensity, extra definitions of dRN and mRN VOIs were delineated by selecting only voxels with >80% uptake within a sphere (diameter of 8mm for the dRN and 6mm for mRN) manually located in these regions, according to visual inspection of the PET image (average of frames 20-23) (subject based, i.e. dRNs and mRNs).

After spatial registration of the images, pharmacokinetic modelling was performed to obtain the [11C]DASB non-displaceable binding potential (BP_{ND}) [17], using the Simplified Reference Tissue Model 2 (SRTM2) [18] with the cerebellum (excluding vermis) as the reference region. BP_{ND} values were obtained from aligned PET images in the individual space for the VOI-based analysis, and in the MNI space for the voxel-based analysis. A Gaussian kernel of 6 mm FWHM was applied to the PET image before voxel-based pharmacokinetic modelling.

Statistical analysis

Statistical analysis was performed using SPSS Statistics 22 (IBM SPSS Statistics, USA). Demographic and clinical data and values obtained from the VOI-based modelling were compared between groups using the Pearson $\chi 2$ test/Fisher's exact test or the Mann-Whitney U test. Differences were considered statistically significant at <5% probability ($p<0.05$) of equality, without correction for multiple comparisons. Additionally, effect sizes were calculated using the Cohen's *d* test, which were interpreted as: $d>0.1$: small effect; $d>0.3$: medium effect; $d>0.5$: large effect [19].

For statistical comparison of the BP_{ND} parametric images a two-sample t-test was performed in SPM12 (Wellcome Trust Centre for Neuroimaging, UK) between dystonia patients and controls. For interpretation of the results, T-maps data were interrogated at $p=0.005$ (uncorrected) and only clusters with $p<0.05$ corrected for family wise error were considered significant.

Correlation analysis between the BP_{ND} obtained from the VOI-based modelling and clinical characteristics was performed using the Spearman's rho test. With multiple regression analysis, we then determined the influence of clinical variables with a *p*-value <0.05 in the univariate analysis on the BP_{ND}. Assumptions of the linear regression and multicollinearity were checked.

RESULTS

Clinical characteristics

14 patients (mean age 56yr, range 46-70) and 14 controls (mean age 54yr, range 39-70) were included in the study (Table 1). Two controls, however, were excluded from the analysis. One healthy control prematurely stopped the scanning procedure. The other subject was excluded due to subcutaneous infusion of the tracer. The patients had a median dystonia duration of 9 years (range 1 – 52) years. The total TWSTRS score was 36.4 (SD ± 15.9), the CGI-S jerks/tremor score 1.9 (SD ± 0.8). Most of the measured NMS scores were significantly higher in the CD patient group as compared with the controls, with values for depression (BDI) of 12.6 (SD ± 6.6) vs. 3.6 (SD ± 3.9) (p<0.01), anxiety (BAI) 8.9 (SD ± 5.6) vs. 3.9 (SD ± 3.6) (p=0.01) and fatigue (FSS) 38.8 (SD ± 14.3) vs. 22.9

Table 1
Demographic and clinical characteristics

	CD (n=14)	Controls (n=12)	Maximum value	Cut-off value	*p*-value
Age	56 ± 9 y	53 ± 8 y			ns
Female	12 (86%)	10 (83%)			ns
Dystonia duration	12 ± 13 y				
TWSTRS					
- Motor severity	17.5 ± 5.7		35		
- Disability	11.6 ± 5.7		30		
- Pain	7.2 ± 6.4		20		
- Total	36.4 ± 15.9		85		
CGI-S tremor/jerks	1.9 ± 0.8		7		
BDI	12.6 ± 6.6	3.6 ± 3.9	63	≥ 10	0.01
BAI	8.9 ± 5.6	3.9 ± 3.6	63	≥ 10	<0.01
FSS	38.8 ± 14.3	22.9 ± 6.6	63	≥ 36	<0.01
PSQI	8.3 ± 3.8	5.3 ± 4.3	21	≥ 5	ns
L_A/L_A genotype	3 (21%)	5 (42%)			ns
Injected dose [^{11}C]DASB (MBq)	387 ± 33.5	371 ± 53			ns

Demographic and clinical characteristics of CD patients and controls, including the maximum values of the different motor and non-motor scales and used cut off values. Data shown as mean ± standard deviation or number (%). CD = cervical dystonia. Y = years. TWSTRS = Toronto Western Spasmodic Torticollis Rating Scale. CGI-S = Clinical Global Impression Scale. BDI = Beck Depression Inventory. BAI = Beck Anxiety Inventory. FSS = Fatigue Severity Scale. PSQI = Pittsburgh Sleep Quality Index.

(SD ± 6.6) (p<0.01). Sleep disturbances (PSQI) were also more severe in CD patients, but the difference did not reach statistical significance: 8.3 (SD ± 3.8) vs. 5.3 (SD ± 4.3) (p=0.16).

The prevalence of the L_A/L_A genotype was not significantly different in patients and controls (42% vs. 21%, p=0.40).

VOI-based analysis of [11C]DASB binding

The distribution of [11C]DASB in control subjects revealed strong binding in the dorsal midbrain, thalamus and striatum (Suppl. figure 1).

No significant differences in the BP_{ND} of SERT between CD patients and controls were detected with the VOI-based analysis (Suppl. table 1). Neither were significant asymmetries detected between the left and right VOIs in any of the groups. The comparison between groups was also performed with both sides combined, providing the same results.
A trend with substantial effect size was detected towards decreased binding in the putamen of CD patients (right 10.7% decrease, d=0.64, p=0.06; left 8.8% decrease, d=0.57, p=0.11) and to a lesser extent in the globus pallidus (right 11.1% decrease, d=0.58, p=0.14; left 5.1% decrease, d=0.20, p=0.50). A trend to an increased binding in the raphe nuclei was found in the patient group as compared to the controls, both in the dRN (dRNs 18.3% increase, d=0.46, p=0.21; dRNa 9.5% increase, d=0.31, p=0.22) and the mRN (mRNs 25.8% increase, d=0.72, p=0.16; mRNa 29.9% increase, d=0.73, p=0.45).

Voxel-based analysis of [11C]DASB binding

Similar to the VOI-based approach, the whole brain voxel-based analysis revealed no significant differences (p=0.005, uncorrected) in the BP_{ND} between CD patients and controls. Exploring the T-maps with a less conservative threshold (p=0.05, uncorrected) the patient group showed a decreased binding bilaterally in the putamen (left T=2.4±0.5; right T=2.2±0.4), left anterior (T=2.2±0.4) and posterior (2.1±0.2) cingulate gyrus, the left superior frontal gyrus (T=2.2±0.4), and the right insula (T=2.1±0.3) (Figure 1, suppl. table 2).

Supplementary figure 1
A representative image of a control subject.

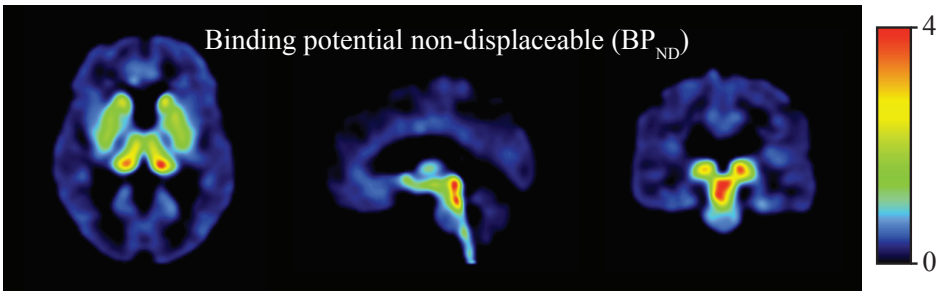

Supplementary table 1

BP_{ND} in CD patients and controls in volumes of interest (VOIs)

	CD (n=14)		Controls (n=12)	
	Right	*Left*	*Right*	*Left*
Thalamus	1.27 ± 0.24	1.22 ± 0.24	1.35 ± 0.23	1.27 ± 0.22
Putamen	1.58 ± 0.30	1.55 ± 0.28	1.77 ± 0.29	1.70 ± 0.25
N. Caudatus	0.78 ± 0.36	1.02 ± 0.50	0.91 ± 0.41	0.87 ± 0.30
G. Pallidus	1.28 ± 0.26	1.50 ± 0.41	1.44 ± 0.29	1.58 ± 0.30
S. Nigra	2.03 ± 0.93	1.90 ± 0.50	1.84 ± 0.27	1.81 ± 0.29
Hippocampus	0.49 ± 0.07	0.49 ± 0.11	0.55 ± 0.12	0.54 ± 0.08
Amygdala	1.51 ± 0.41	1.65 ± 0.44	1.70 ± 0.44	1.61 ± 0.40
Anterior cingulate cortex	0.43 ± 0.09	0.42 ± 0.08	0.47 ± 0.08	0.48 ± 0.10
Frontal cortex				
- Middle- and inferior frontal gyrus	0.23 ± 0.06	0.22 ± 0.07	0.25 ± 0.07	0.24 ± 0.06
- Superior frontal gyrus	0.16 ± 0.05	0.17 ± 0.06	0.19 ± 0.05	0.19 ± 0.06
- Anterior-, medial-, lateral- and posterior orbital gyrus	0.28 ± 0.09	0.32 ± 0.08	0.31 ± 0.04	0.35 ± 0.06
- Subgenual frontal cortex, subcallosal area and pre-subgenual frontal cortex	0.63 ± 0.16	0.60 ± 0.13	0.67 ± 0.10	0.60 ± 0.13
Cuneus + lingual gyrus	0.36 ± 0.09	0.35 ± 0.09	0.35 ± 0.08	0.36 ± 0.10
Insula	0.62 ± 0.11	0.61 ± 0.11	0.69 ± 0.10	0.67 ± 0.12
Temporal lobe	0.22 ± 0.06	0.22 ± 0.07	0.55 ± 0.05	0.23 ± 0.05
dRN				
- dRNa	5.29 ± 1.32		4.79 ± 1.84	
- dRNs	6.78 ± 1.62		5.54 ± 3.42	
mRN				
- mRNa	9.67 ± 5.08		6.78 ± 2.28	
- mRNs	10.02 ± 4.76		7.43 ± 1.72	

The BPND of the different volumes of interest in CD patients and controls. No significant differences were detected. Data are shown as mean ± standard deviation. CD = cervical dystonia. BPND = binding potential, non-displaceable. dRN = dorsal raphe nucleus, atlas based (dRNa) or subject based (dRNs). mRN = median raphe nucleus, atlas based (mRNa) or subject based (mRNs).

Correlations between clinical variables and [^{11}C]DASB binding.

In CD patients, motor symptom severity was significantly correlated with the BP_{ND} in the dRN (dRNs: r_s=0.65, p=0.01; dRNa: r_s=0.60, p=0.02). No other regions, particularly not the basal ganglia, showed such a correlation with motor symptom severity. Among the NMS scores, we found a significant correlation between the BP_{ND} in the dRN and pain (dRNs: r_s=0.73, p<0.01; dRNa: r_s=0.58, p=0.03) and sleep disturbances (dRNs: r_s=0.73, p<0.01, dRNa: r_s=0.71, p<0.01) (Figure 2, suppl. table 3). Patients with the L_A/L_A genotype had a relatively low BP_{ND} in the dRNs, namely 5.1, 5.2 and 5.4.

Subsequently, in the multiple regression analysis, we included motor symptom severity, pain and sleep disturbances to assess the effect on the BP_{ND} of the dRNs. As there was multicollinearity between pain and sleep disturbances scores (r_s=0.87, p<0.01), this was performed in two separate steps. First, we included motor severity and pain in the

Figure 1
Results of the voxel-based analysis.

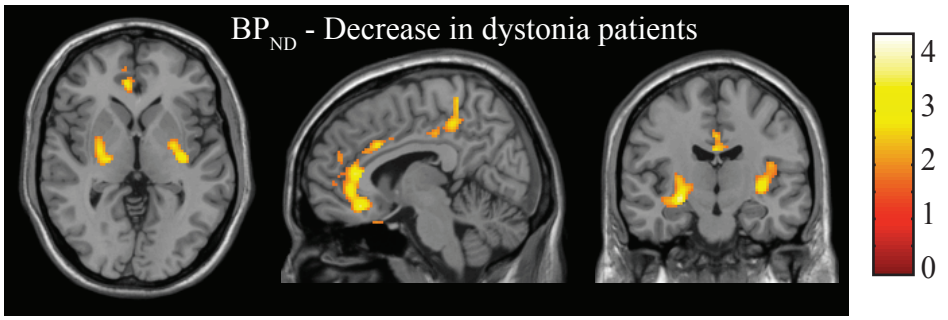

Regions with a decreased BPND (voxel-threshold of p=0.05, uncorrected) in CD patients compared with controls.

Supplementary table 2
Decreased BP_{ND} in CD patients compared with controls.

Region	*Voxels*	*T*	±	*SD*	*Cohen's d*
Cingulate gyrus anterior part left	247	2.18	±	0.39	0.89
Cingulate gyrus posterior part left	167	2.07	±	0.24	0.84
Putamen left	151	2.39	±	0.51	0.98
Putamen right	119	2.21	±	0.41	0.90
Insula right	225	2.11	±	0.32	0.86
Superior frontal gyrus left	165	2.20	±	0.44	0.90

Functional regions (>100 voxels) showing a decreased BPnd, obtained from significant clusters when the T-maps were explored with a p=0.05 uncorrected threshold and a minimum cluster size of 400. For each functional region, the mean T-value, standard deviation (SD), effect size (Cohen's d), and voxel size are reported. BPND = binding potential, non-displaceable. CD = cervical dystonia.

model. This revealed an adjusted R^2 of 0.47; none of the variables significantly influenced the model. Second, we included motor symptom severity and sleep disturbances in the model. This revealed an adjusted R^2 of 0.55, with motor symptom severity being the most important predictor of an increased BP_{ND} in the dRNs (β=1.56, p=0.02) (Table 2).
Furthermore, fatigue was associated with a decreased BP_{ND} in the mRN (mRNs: r_s=-0.61, p=0.045, mRNa: r_s=-0.63, p=0.049); while depression (r_s=-0.54, p=0.045) and anxiety (r_s=-0.55, p=0.04) showed an association with a decreased BP_{ND} in only the right hippocampus.

Figure 2
Correlation between the BP_{ND} in the dRNs in CD patients and clinical variables.

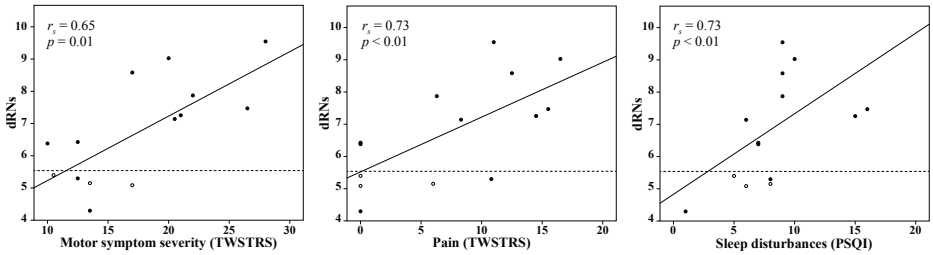

Univariate correlation analysis in CD patients between the BP_{ND} in the dRNs and the TWSTRS motor severity score, TWSTRS pain score and PSQI score. The dashed line indicates the mean BP_{ND} in the dRNs of the control group. Patients with the L_A/L_A genotype are indicated as white circles. BP_{ND} = binding potential, non-displaceable. dNRs: dorsal raphe nucleus, subject based. CD = cervical dystonia. r_s = Spearman's rho. TWSTRS = Toronto Western Spasmodic Torticollis Rating Scale. PSQI = Pittsburgh Sleep Quality Index.

Supplementary table 3
Univariate correlation analysis between the BP_{ND} in the dRNs in CD patients and clinical variables.

	TWSTRS severity	TWSTRS pain	BDI	BAI	FSS	PSQI
dRNs	0.65**	0.73**	-0.41	-0.20	-0.13	0.73**
TWSTRS severity		0.67**	-0.41	-0.29	-0.05	0.64*
TWSTRS pain			-0.17	-0.11	0.05	0.87**
BDI				0.51	0.65*	-0.24
BAI					0.15	-0.11
FSS						-0.02

Data are shown as correlation coefficient. BP_{ND} = binding potential, non-displaceable. dRNs: dorsal raphe nucleus, subject based. *p<0.05, **p<0.01. TWSTRS = Toronto Western Spasmodic Torticollis Rating Scale. BDI = Beck Depression Inventory. BAI = Beck Anxiety Inventory. FSS = Fatigue Severity Scale. PSQI = Pittsburgh Sleep Quality Index.

Table 2
Multiple regression analysis between the BP_{ND} of the dRNs and clinical variables.

Model	Region	Predictors	Adjusted R Square	B°	β	p-value
1	dRNs	- TWSTRS severity	0.47	0.10 (0.14)	0.34	0.49
		- TWSTRS pain		0.02 (0.22)	0.10	0.91
		- Interaction effect		0.00 (0.01)	0.38	0.75
2	dRNs	- TWSTRS severity	0.55	0.44 (0.16)	1.56	0.02
		- PSQI		0.70 (0.35)	1.65	0.07
		- Interaction effect		-0.03 (0.02)	-2.21	0.09

Results of the multiple regression analysis to assess the effect of the TWSTRS severity score, the TWSTRS pain score, the PSQI score and additional interaction effects on the BP_{ND} in the dRNs in CD patients. Due to multicollinearity between the TWSTRS pain score and PSQI score, we performed the analysis in two separate steps. For all variables, we calculated the B° (unstandardized coefficient with standard error in parenthesis) and β (standardized regression coefficient). BP_{ND} = binding potential, non-displaceable. dRNs: dorsal raphe nucleus, subject based. TWSTRS = Toronto Western Spasmodic Torticollis Rating Scale. PSQI = Pittsburgh Sleep Quality Index.

DISCUSSION

In this functional brain imaging study, we demonstrated a significant correlation between increased [11C]DASB SERT binding in the dRN of CD patients and the severity of dystonic motor symptoms, pain and sleep disturbances, respectively, but not with psychiatric co-morbidity. This correlation of clinical parameters with increased binding in the dRN is consistent with the observed trend of increased SERT binding in this midbrain center of serotonin neurons in CD when compared to controls. At the hemisphere target regions of serotonin innervation, we found a trend towards a bilateral decrease of SERT binding in the putamen and pallidum. These opposite trends may illustrate the dynamic complexity of serotonin neurotransmitter regulation.

For the interpretation of our results, it is important to keep in mind that, although the level of regionally measured [11C]DASB generally reflects the available SERT binding sites, this binding may be influenced by the quantity of endogenous serotonin, competing at the binding sites. E.g., an increase of endogenous serotonin may reduce [11C]DASB binding without a change in the actual number of binding sites. The latter has particularly been demonstrated in acute experimental conditions of drugs employed to manipulate serotonin availability [20]. As the patients included in our study were characterized by a distinct profile of symptoms, the finding of a significant correlation between symptom severity and increased dRN [11C]DASB binding provides a strong argument to regard this dRN binding as a fair index of the actual SERT binding sites in the participating subjects. The concept of increased serotonergic activity in CD is supported by the literature describing serotonin-induced motor effects. In both cat and monkey, serotonin injections

in the facial nucleus induced focal dystonia of the eyelids [21]. Administering the precursor of serotonin elicits a consistent hyperkinetic motor syndrome including lateral head waving [22]. At the spinal cord level, serotonin increases spinal motor neuron excitability, facilitating the generation of action potentials [23]. Moreover, serotonergic activation caused suppression of sensory information processing [24], which is compatible with the disturbed sensorimotor (afferent) integration known to be an important key stone of the dystonia pathophysiology [4].

Although direct effects of serotonin injections in the basal ganglia have not been investigated, the strong increase of endogenous serotonin release in the monkey striatum by a precursor challenge [20], highlights the functional interrelationship of the basal ganglia with the origin of serotonergic innervation in the dRN and underscores that changed serotonergic activity in the putamen and globus pallidus is consistent with the current hypothesis concerning their involvement in the pathophysiology underlying dystonia [3,4]. Dyskinesia is another condition of increased motor activity, occurring in Parkinson's disease and associated with an increased ratio of serotonergic versus dopaminergic putamen innervation [6]. Finally, coherent change of serotonin activity in the basal ganglia and the raphe nucleus has recently been described in social anxiety disorder, in which increased [^{11}C]DASB binding in the two regions was explained by presynaptic serotonergic overactivity [25].

The trend of decreased [^{11}C]DASB binding in the basal ganglia of our CD patients, which we explained as a result of increased endogenous serotonin release, did not reach statistical significance. Given the medium to large effect size, one may argue that this absence of significance was due to a small sample size. Nevertheless, the subthreshold identification of bilateral striatum decreases in [^{11}C]DASB binding resulted from both pre-defined VOI and hypothesis-free voxel-based analyses. Particularly the distinct spatial pattern that emerged from the latter supports our inference that this changed [^{11}C]DASB binding indeed represents region-specific serotonergic changes within the cerebral hemispheres of CD patients.

To illustrate the complexity of the balance between serotonergic activity in the dRN and basal ganglia, a full review of the entire spectrum of regulatory mechanisms in cerebral serotonin activity would be required, which is, however, beyond the scope of this paper. We only mention that e.g. increased 5-HT$_{1A}$ autoreceptor activation in the dRN may have an inhibitory effect on discharge patterns to the output areas [26]. In Parkinson's disease, such reduced serotonergic activity in the basal ganglia by stimulating inhibitory 5-HT$_{1A}$ receptors may ameliorate dyskinesia [6]. These circumstances of increased SERT binding in the dRN together with decreased striatum SERT binding may reflect an adaptive mechanism. As we found a correlation between increased symptom severity and increased dRN and not with decreased striatum binding, we regard increased SERT binding in the dRN to be a primary and not an adaptive effect. The above discussed

issues indeed point at the limitation of [11C]DASB as a tracer that only provides detailed information about serotonin transporter binding, but not about other serotonergic receptors and the interaction with other neurotransmitters. Future combined studies of SERT and 5-HT_{1A} autoreceptor binding and/or with other postsynaptically located receptors or different neurotransmitters would potentially provide more insight in the dynamic balance of serotonergic functioning.

Not only motor severity but also pain and sleep disturbances showed a positive correlation with the BP_{ND} in the dRN. Serotonin involvement in pain is supported by previous studies. For example, spinal analgesic action is mediated by serotonin release, and selective serotonin reuptake inhibitors induce a central analgesic effect [27]. In sleep disorders, altered discharge patters of serotonergic neurons were suggested to be involved by influencing the different serotonergic postsynaptic receptors [28]. Altogether, the relation between SERT binding in the dRN and motor severity, pain and sleep disturbances supports our hypothesis that serotonin forms a shared pathophysiological pathway of motor and NMS in dystonia.

Depression and anxiety were not related to the BP_{ND} in the dRN, but were significantly related to a decreased BP_{ND} in the right hippocampus. The lack of correlation between the dRN and psychiatric features is difficult to compare with previous studies as raphe values in those studies were measured as part of the whole brainstem region (including other nuclei) or not reported at all. Our findings in CD with reductions in the hippocampus-amygdala complex are in line with previous studies in depressive patients (for meta-analyses see Kambeitz and Howes [29] and Meyer [30]). Whether these SERT binding reductions in limbic regions underlies vulnerability to depression or represent a psychopathological state (state or trait factor) is unclear in both the depression studies and in our CD cohort. Longitudinal studies and larger and more heterogeneous samples will be required for further clarification.

In conclusion, this study provides evidence on involvement of the serotonergic system in both motor and NMS in CD, which motivates the design of future studies with serotonergic drugs on the motor and NMS symptoms in CD, if possible combined with the effect on receptor binding imaging, thus opening a new therapeutic field for dystonia patients.

Supplementary text: SERT genotyping

The SERT S/L_A/L_G variants were determined using polymerase chain reaction (PCR) with Forward primer FAM-5'TGAATGCCAGCACCTAACCC-3' and Reverse primer 5-TTCTGGTGCCACCTAGACGC-3', and subsequent ingestion of the PCR product with Msp-I for at least 3 hours at 37 °C. The resulting restriction fragments were separated using capillary electrophoresis (ABI 3130 analyzer; Applied Biosystems, the Netherlands) and fragment sizes were estimated using the ABI Prism® GeneMapper™ software, version 3.0 (Applied Biosystems). The S, L_G and L_A variants were determined by detection of fragments of 325, 152 or 284 base pairs, respectively.

REFERENCES

[1] L. Klingelhoefer, D. Martino, P. Martinez-Martin, A. Sauerbier, A. Rizos, W. Jost, T.T. Warner, K.R. Chaudhuri, Non-motor symptoms and focal cervical dystonia: observations from 102 patients, 4(3-4):117-120. (2014). doi:10.1016/j.baga.2014.10.002.

[2] M. Smit, A.L. Bartels, M. van Faassen, A. Kuiper, K.E. Niezen-Koning, I.P. Kema, R.A. Diercks, T.J. de Koning, M.A. Tijssen, Serotonergic perturbations in dystonia disorders-a systematic review, Neurosci. Biobehav. Rev. 65 (2016) 264–275. doi:S0149-7634(15)30152-4 [pii].

[3] M. Vidailhet, M.F. Jutras, D. Grabli, E. Roze, Deep brain stimulation for dystonia, J. Neurol. Neurosurg. Psychiatry. 84 (2013) 1029–1042. doi:10.1136/jnnp-2011-301714 [doi].

[4] A. Quartarone, M. Hallett, Emerging concepts in the physiological basis of dystonia, Mov. Disord. 28 (2013) 958–967. doi:10.1002/mds.25532 [doi].

[5] C. Loane, K. Wu, P. Bain, D.J. Brooks, P. Piccini, M. Politis, Serotonergic loss in motor circuitries correlates with severity of action-postural tremor in PD, Neurology. 80 (2013) 1850–1855. doi:10.1212/WNL.0b013e318292a31d [doi].

[6] J.Y. Lee, S. Seo, J.S. Lee, H.J. Kim, Y.K. Kim, B.S. Jeon, Putaminal serotonergic innervation: monitoring dyskinesia risk in Parkinson disease, Neurology. 85 (2015) 853–860. doi:10.1212/WNL.0000000000001909 [doi].

[7] N. Pavese, V. Metta, S.K. Bose, K.R. Chaudhuri, D.J. Brooks, Fatigue in Parkinson's disease is linked to striatal and limbic serotonergic dysfunction, Brain. 133 (2010) 3434–3443. doi:10.1093/brain/awq268 [doi].

[8] M. Politis, K. Wu, C. Loane, F.E. Turkheimer, S. Molloy, D.J. Brooks, P. Piccini, Depressive symptoms in PD correlate with higher 5-HTT binding in raphe and limbic structures, Neurology. 75 (2010) 1920–1927. doi:10.1212/WNL.0b013e3181feb2ab [doi].

[9] E.S. Consky, A.E. Lang, Clinical assessments of patients with cervical dystonia. In: Jankovic J, Hallett M, editors. Therapy with botulinum toxin. New York, NY: Marcel Dekker, (1994) 211–237.

[10] W. Guy, The Clinical Global Impression scale. In: ECDEU Assessment Manual for Psychopharmacology-Revised. Rockville, MD: US Dept. of Health, Education and Welfare, ADAMHA, NIMH Psychopharmacology Research Branch, (1976) 218. doi:222.

[11] M. Smit, A. Kuiper, V. Han, V.C. Jiawan, G. Douma, B. van Harten, J.M.T.H. Oen, M.E. Pouwels, H.J.G. Dieks, A.L. Bartels, M.A. Tijssen, Psychiatric co-morbidity is highly prevalent in idiopathic cervical dystonia and significantly influences health-related quality of life: Results of a controlled study, Parkinsonism Relat. Disord. (2016). doi:S1353-8020(16)30216-4 [pii].

[12] X.Z. Hu, R.H. Lipsky, G. Zhu, L.A. Akhtar, J. Taubman, B.D. Greenberg, K. Xu, P.D. Arnold, M.A. Richter, J.L. Kennedy, D.L. Murphy, D. Goldman, Serotonin transporter promoter gain-of-function genotypes are linked to obsessive-compulsive disorder, Am. J. Hum. Genet. 78 (2006) 815–826. doi:S0002-9297(07)63816-6 [pii].

[13] A.A. Wilson, N. Ginovart, M. Schmidt, J.H. Meyer, P.G. Threlkeld, S. Houle, Novel radiotracers for imaging the serotonin transporter by positron emission tomography: synthesis, radiosynthesis, and in vitro and ex vivo evaluation of (11) C-labeled 2-(phenylthio)araalkylamines, J. Med. Chem. 43 (2000) 3103–3110. doi:jm000079i [pii].

[14] J. Ashburner, K.J. Friston, Unified segmentation, Neuroimage. 26 (2005) 839–851. doi:S1053-8119(05)00110-2 [pii].

[15] A. Hammers, R. Allom, M.J. Koepp, S.L. Free, R. Myers, L. Lemieux, T.N. Mitchell, D.J. Brooks, J.S. Duncan, Three-dimensional maximum probability atlas of the human brain, with particular reference to the temporal lobe, Hum. Brain Mapp. 19 (2003) 224–247. doi:10.1002/hbm.10123 [doi].

[16] G.S. Kranz, A. Hahn, M. Savli, R. Lanzenberger, Challenges in the differentiation of midbrain raphe nuclei in neuroimaging research, Proc. Natl. Acad. Sci. U. S. A. 109 (2012) E2000. doi:10.1073/pnas.1206247109 [doi].

[17] R.B. Innis, V.J. Cunningham, J. Delforge, M. Fujita, A. Gjedde, R.N. Gunn, J. Holden, S. Houle, S.C. Huang, M. Ichise, H. Lida, H. Ito, Y. Kimura, R.A. Koeppe, G.M. Knudsen, J. Knuti, A.A. Lammertsma, M. Laruelle, J. Logan, R.P. Mauire, M.A.Mintun, E.D. Morris, R. Parsey, J.C. Price, M. Slifstein, V. Sossi, T. Suhara, J.R.

Votaw, D.F. Wong, R.E Carson, Consensus nomenclature for in vivo imaging of reversibly binding radioligands, J. Cereb. Blood Flow Metab. 27 (2007) 1533–1539. doi:9600493 [pii].

[18] Y. Wu, R.E. Carson, Noise reduction in the simplified reference tissue model for neuroreceptor functional imaging, J. Cereb. Blood Flow Metab. 22 (2002) 1440–1452. doi:10.1097/00004647-200212000-00004 [doi].

[19] A. Field, Discovering statistics using SPSS, SAGE Publications, 2009.

[20] S. Yamamoto, H. Onoe, H. Tsukada, Y. Watanabe, Effects of increased endogenous serotonin on the in vivo binding of [11C]DASB to serotonin transporters in conscious monkey brain, Synapse. 61 (2007) 724–731. doi:10.1002/syn.20422 [doi].

[21] M.S. LeDoux, J.F. Lorden, J.M. Smith, L.E. Mays, Serotonergic modulation of eye blinks in cat and monkey, Neurosci. Lett. 253 (1998) 61–64. doi:S0304-3940(98)00616-8 [pii].

[22] B.L. Jacobs, C.A. Fornal, 5-HT and motor control: a hypothesis, Trends Neurosci. 16 (1993) 346–352.

[23] J.F. Perrier, Modulation of motoneuron activity by serotonin, Dan. Med. J. 63 (2016) B5204. doi:B5204 [pii].

[24] B.L. Jacobs, C.A. Fornal, Serotonin and motor activity, Curr. Opin. Neurobiol. 7 (1997) 820–825. doi:S0959-4388(97)80141-9 [pii].

[25] A. Frick, F. Ahs, J. Engman, M. Jonasson, I. Alaie, J. Bjorkstrand, O. Frans, V. Faria, C. Linnman, L. Appel, K. Wahlstedt, M. Lubberink, M. Frederison, T. Furmark, Serotonin Synthesis and Reuptake in Social Anxiety Disorder: A Positron Emission Tomography Study, JAMA Psychiatry. 72 (2015) 794–802. doi:10.1001/jamapsychiatry.2015.0125 [doi].

[26] E. Sibille, D.A. Lewis, SERT-ainly Involved in Depression, But When?, Am J Psychiatry 1631, January 2006. (2006) 8.

[27] C. Sommer, Serotonin in pain and analgesia: actions in the periphery, Mol. Neurobiol. 30 (2004) 117–125. doi:MN:30:2:117 [pii].

[28] C.M. Portas, B. Bjorvatn, R. Ursin, Serotonin and the sleep/wake cycle: special emphasis on microdialysis studies, Prog. Neurobiol. 60 (2000) 13–35. doi:S0301-0082(98)00097-5 [pii].

[29] J.P. Kambeitz, O.D. Howes, The serotonin transporter in depression: Meta-analysis of in vivo and post mortem findings and implications for understanding and treating depression, J. Affect. Disord. 186 (2015) 358–366. doi:10.1016/j.jad.2015.07.034 [doi].

[30] J.H. Meyer, S. Houle, S. Sagrati, A. Carella, D.F. Hussey, N. Ginovart, V. Goulding, J. Kennedy, A.A. Wilson, Brain serotonin transporter binding potential measured with carbon 11-labeled DASB positron emission tomography: effects of major depressive episodes and severity of dysfunctional attitudes, Arch. Gen. Psychiatry. 61 (2004) 1271–1279. doi:61/12/1271 [pii].